Agricultural Water Management 221 (2019) 131–140

Contents lists available at ScienceDirect

Agricultural Water Management

journal homepage: www.elsevier.com/locate/agwat

# Assessing the impact of climate change on rainwater harvesting in the Oum Zessar watershed in Southeastern Tunisia

Ammar Adham[a,c,*], Jan G. Wesseling[a], Rasha Abed[a], Michel Riksen[a], Mohamed Ouessar[b], Coen J. Ritsema[a]

[a] Wageningen University, Soil Physics and Land Management Group, P.O. Box 47, 6700 AA, Wageningen, the Netherlands
[b] Institut des Régions Arides, Route de Djorf km22.5, 4119, Medenine, Tunisia
[c] Department of Civil Engineering, Engineering college, University of Anbar, Ramadi, Iraq

ARTICLE INFO

*Keywords:*
Climate change
GCMs
SDSM
Water harvesting model
Tunisia

ABSTRACT

Climate change is believed to have a large impact on water resources system both globally and regionally. It has become a major global issue, especially in developing countries because these are most affected by its impacts. Rainwater harvesting techniques offer an alternative source of water and represent specific adaptive strategies to cope with water scarcity within future climate change. Studying the impact of climate change on rainwater harvesting techniques, however, is difficult, because the general circulation models (GCMs) which are widely used to simulate scenarios of future climate change operate on a coarse scale. We estimated the impact of climate change on water availability at the watershed level by downscaling precipitation and temperature from the GCMs using a statistical downscaling model. A water harvesting model then assessed the performance of the rainwater harvesting techniques for the Oum Zessar watershed in southeastern Tunisia under current climatic conditions and scenarios of future climate change. Annual temperature tended to increase and precipitation tended to decrease. These changes of climatic variables were used in the water harvesting model to simulate future water availability. Changing the directions of water flow between sub-catchments in combination with changing the spillway heights strongly affected the performance of rainwater harvesting under the scenarios of future climate, resulting in a sufficient water supply for 92% of all sub-catchments, compared to 72% without these changes.

## 1. Introduction

Arid and semi-arid regions (ASARs) around the world are facing serious challenges of water availability. Climate change is a very serious phenomenon and has become a major global issue in recent years, especially in developing countries strongly affected by its impacts. Multiple climate models predict that climate change would amplify the intensity and frequency of droughts and thus decrease water availability, particularly in semiarid regions (Li et al., 2018). The United Nations Framework Convention on Climate Change defines climate change as *"a change of climate which is attributed directly or indirectly to human activity that alters the composition of the global atmosphere and which is in addition to natural climate variability observed over comparable time periods"* (www.unfccc.int). The Intergovernmental Panel on Climate Change (IPCC, 2014b) predicts that the global mean surface temperature will probably increase by 0.3 – 0.7 °C during 2016–2035 and by 2.6–4.8 °C during 2081–2100. Higher temperatures lead to higher evaporation rates, to a higher frequency of droughts and to reductions in streamflow (Rind et al., 1990). Tunisia is amongst the lowest water-use countries (450 $m^3$/capita/y) and amongst the most vulnerable to the effects of climate change (MARH, 2011). Climatic projections applied to Tunisia have shown that the average temperature will increase by 1.1 °C by 2030 and by 2.1 °C by 2050. Combining these numbers with a decrease of rainfall, which is predicted to be between 10% in the north and 30% in the south during the same period (MARH, 2011), suggests that Tunisia will face a scarcity of water.

Inhabitants of ASARs are adapting rainwater harvesting (RWH) techniques to provide an alternative source of water to meet the increasing demand (Ammar et al., 2016). RWH represents a specific adaptive strategy to cope with water scarcity and future climate change (Mukheibir, 2008). Climatic variables and scenarios of climate change must be developed on a regional or even site-specific scale to ensure the success and sustainability of adapting RWH techniques to the impacts of climate change (Wilby and Wigley, 2000). Projections of climatic

* Corresponding author at: Wageningen University, Soil Physics and Land Management Group, P.O. Box 47, 6700 AA, Wageningen, the Netherlands.
*E-mail addresses:* ammar.ali@wur.nl, engammar2000@uoanbar.edu.iq, engammar2000@uoanbar.edu.iq (A. Adham).

https://doi.org/10.1016/j.agwat.2019.05.006
Received 3 December 2018; Received in revised form 13 April 2019; Accepted 1 May 2019

variables must be 'downscaled' from the results of general circulation models (GCMs) to provide these values, i.e. the climatic projections should be translated from coarse-resolution GCMs to finer resolutions using either dynamic or statistical methods (Ipcc-Tgic, 2007).

Different methodologies can assess the impact of climate change on RWH, water availability, runoff, and water balance within large catchments (Chiew et al., 1995), but only a few studies have focused on small sub-catchments. Abouabdillah (2010) applied the SWAT2005 model to study the impact to central Tunisia of three scenarios of future climates, generated with the Canadian Global Coupled Model (CGCM 3.1). The data for precipitation and temperature were generated using statistically downscaling of the CGCMs, and the potential impact of climate change on flow, evapotranspiration, and soil moisture across this catchment was analysed. Al-Ansari et al. (2014) tested the projected validity of RWH techniques in the Iraqi province of Sulaimaniyah using data based on global climatic projections provided by the HadCM3 GCM.

Climatic and hydrological models have not supplied adaptive strategies for optimising RWH effectiveness in ASARs. Analysing the performance and efficiency of RWH techniques for the collection, storage and use of the scarce water is therefore necessary. The potential redesign of RWH structures to adapt to future conditions requires more study as well. We developed a tool to assess the performance of existing RWH techniques and to improve the design of the RWH structures (Adham et al., 2016b).

The main objective of the present study was to investigate the impact of climate change on RWH by assessing the performance of current RWH systems for our case-study area, the Oum Zessar watershed in southeastern Tunisia, under different climatic scenarios. Potential adaptive strategies for optimising RWH effectiveness to mitigate the impact of the predicted climate change were also investigated.

## 2. Materials and methods

### 2.1. Study area and data used

The Oum Zessar watershed in the province of Medenine in southeastern Tunisia covers an area of 367 $km^2$. A 50-ha catchment in the upstream area of the watershed was selected for this case study. This catchment consists of 25 sub-catchments (Fig. 1). The area is characterised by an arid Mediterranean climate with a rainfall of 150–230 mm/y, an annual temperature of 19–22 °C, and a potential evapotranspiration of 1450 mm/y (Adham et al., 2016a).

Local farmers have built two main types of RWH structures to cope with water scarcity and to harvest rainfall/runoff for satisfying the water requirements of rainfed crops and trees: jessour (in areas with moderate to steep slopes) and tabias (in gently sloping foothills)

Two types of data were required for our study. The first type was used for downscaling and modelling climate change. Daily precipitation, maximum temperature and minimum temperature data were collected from two nearby meteorological stations, at the Institute des Régions Arides (*IRA*) and Medenine/Tunisia. Daily data for large-scale predictor variables representing current climatic conditions (1961–2005) were derived by reanalysing the data from the National Centres for Environmental Prediction (NCEP) and the National Centre for Atmosphere Research (NCAR). The NCEP data were downloaded from the Canadian Climate Data and Scenarios website http://ccds-dscc.ec.gc.ca/.

The second type of data consisted of the input data for the water harvesting model (WHCatch) (Adham et al., 2016b). To gather these data, physical characteristics of each sub-catchment under consideration were measured. Soil texture was obtained by collecting samples, and the slope of the area was determined in each sub-catchment using a digital elevation model (DEM) and a geographic information system (GIS). Rates of infiltration were measured in the field using a double-ring infiltrometer and the runoff coefficients were measured using a rainfall simulator at a number of locations in each sub-catchment (Adham et al., 2016b).

### 2.2. Methodology overview

The impacts of climate change on the effects of the RWH techniques were assessed by:

1 Applying GCMs to simulate climatic variables at a large scale and to project scenarios of future global climate.
2 Downscaling the large-scale meteorological variables to local scales.
3 Using the WHCatch model to simulate the effects of climate change on the RWH techniques and to optimise the RWH structures to mitigate the impact of the change.

#### 2.2.1. GCMs and climate change scenarios

The fifth phase of the Coupled Model Intercomparison Project (CMIP5) started releasing GCM climate-change data in 2011, encompassing simulations from more than 20 research groups and 50 models (Lebel et al., 2015). GCMs are numerically coupled models representing various earth systems, including the atmosphere, oceans, land surface, and sea ice. GCMs are generally used to simulate the present climate and to project future climate with forcing by greenhouse gases and aerosols (Dibike and Coulibaly, 2005). The GCMs were primarily developed in 1956 to simulate average, synoptic-scale patterns of atmospheric circulation, but various other GCMs have been designed and developed since for forecasting the weather, understanding the climate, and predicting future climate changes (Xu, 1999). We used only one model, the second-generation Canadian Earth System Model (CanESM2). CanESM2 has been commonly used for various regions. It was developed by the Canadian Centre for Climate Modelling and Analysis (CCCma) of Environment Canada. We used CanESM2 because it is the only model that produces daily predictor variables that can be directly applied to the Statistical DownScaling Model (SDSM). CanESM2 was prepared for CMIP5 basically as the contribution to IPCC's fifth assessment report (AR5) (Taylor et al., 2012). CCCma provided the NCEP/NCAR predictor variables in addition to the large-scale atmospheric variables from CanESM2 for the same period (1961–2005) and also the same variables. Both the NCEP/NCAR and CanESM2 data were downloaded from the Canadian Climate Data and Scenarios website http://ccds-dscc.ec.gc.ca/. The CanESM2 outputs were downloaded for three climatic scenarios, Representative Concentration Pathway (RCP) 2.6, RCP 4.5, and RCP 8.5, which were used in this study. These scenarios were developed and used recently for preparing AR5. The RCP 2.6, was developed by the IMAGE modelling team of the PBL Netherlands Environmental Assessment Agency. The RCP 2.6 is a representative for scenarios in the literature leading to very low greenhouse gas concentration levels (Van Vuuren et al., 2011). The RCP 4.5 was developed by the GCAM modelling group at the Pacific Northwest National Laboratory's Joint Global Change Research Institute (JGCRI) in the United States. It is a stabilization scenario where total radiative forcing is stabilized before 2100 by employment of a range of technologies and strategies for reducing greenhouse gas emissions (Rajesh, 2015). The RCP 8.5 was developed by the MESSAGE modelling team and the Integrated Assessment Framework at the International Institute for Applied System Analysis (IIASA) in Austria. The RCP 8.5 is characterized by increasing greenhouse gas emissions over time representating those scenarios in the literature which lead to high greenhouse gas concentration levels (Thomson et al., 2011). Climatic scenarios refer to plausible future climates; they are images of the future or an alternative future (Setegn et al., 2011). Climatic scenarios have become an important element in research on climate change, because they allow us to understand the long-term consequences and describe plausible pathways of future climatic conditions (Moss et al., 2010). Daily data for precipitation and maximum and minimum temperature were extracted from CanESM2 to be used in the WHCatch

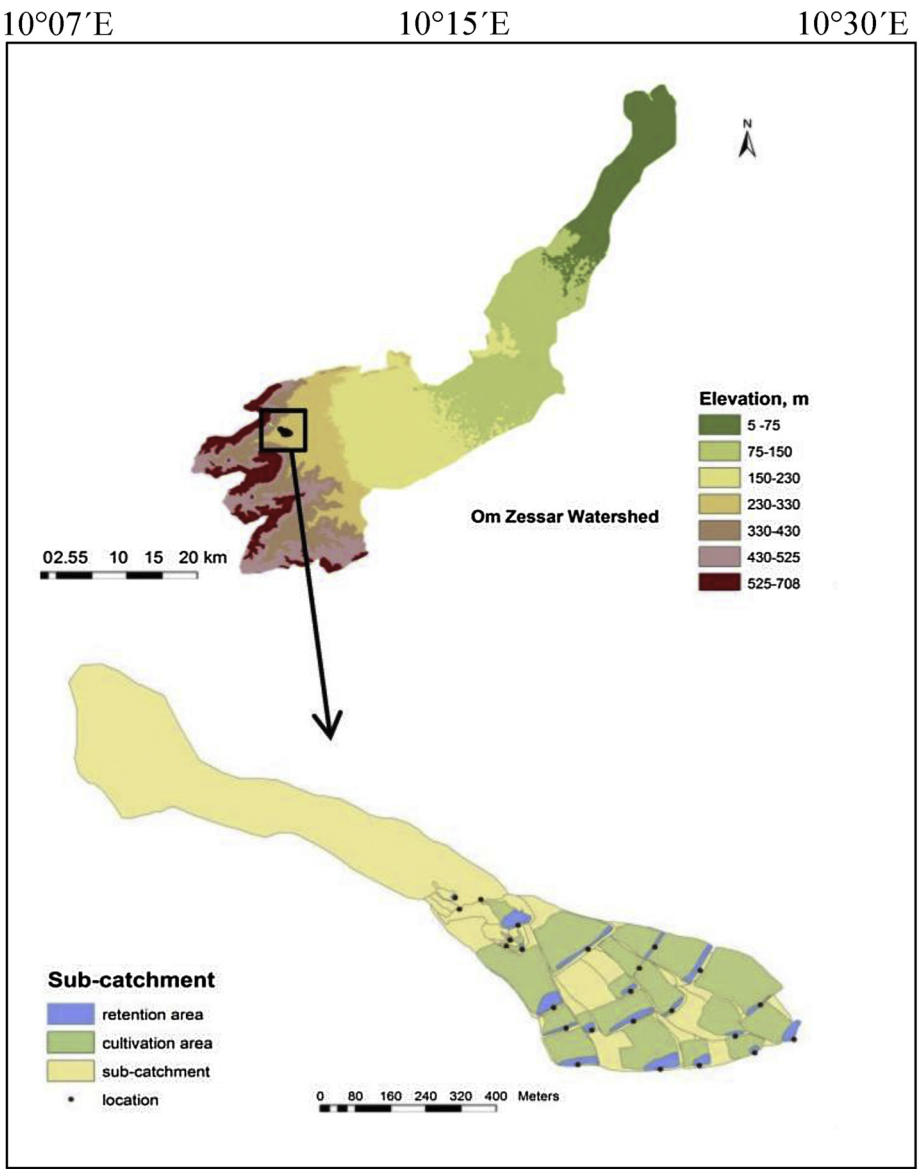


**Fig. 1.** Location of wadi Oum Zessar watershed and the test sub-catchment. The location for each rainwater harvesting structure with its retention area and cultivation area are presented as well.

model to assess the impact of climate change on RWH for the three scenarios RCP 2.6, 4.5, and 8.5.

### 2.2.2. Downscaling methods

GCMs are coarse in resolution and are unable to resolve important sub-grid-scale features such as topography and land use (Grotch and MacCracken, 1991). There is a large gap between the coarse resolution of GCMs and the local watershed processes (Setegn et al., 2011). GCMs were not designed for studying the impact of climate change on a local scale and do not provide direct estimates of hydrological responses to climate change (Dibike and Coulibaly, 2005). A hydrological model is therefore necessary for studying the impacts of climate change on sub-grid scales. Hydrological models need data at similar to sub-grid scales, so the methods used to translate GCM outputs into local meteorological variables required for reliable hydrological modelling are referred to as 'downscaling' techniques (Dibike and Coulibaly, 2005). Dynamic and statistical downscaling are the two main approaches available for downscaling the results of computations by GCMs. The statistical approach, as used in this study, establishes empirical relationships between local climatic variables (predictands) and large-scale atmospheric variables (predictors). Statistical downscaling is less technically demanding than original modelling, computationally cheaper, and can tailor scenarios for specific localities, scales, and problems (Setegn et al., 2011). The main drawback is the assumption that the statistical relationships developed for the present climate also hold under the different forcing conditions of a possible future climate (Abdo et al., 2009).

Formally, the concept of conditioning the regional climate by the large-scale state may be written as:

$$R = F(L) \quad (1)$$

where R is the predictand, L is the predictor (a set of large-scale climatic variables), and F is a deterministic/stochastic function conditioned by L that must be derived empirically from historical observations or modelled data sets (Dibike and Coulibaly, 2005).

*2.2.2.1. Statistical downscaling model (SDSM 4.2).* SDSM is a statistical downscaling tool widely applied in climatic studies. It is a hybrid model that uses linear regression and a stochastic weather generator (Hassan et al., 2014). It is a decision support tool developed by Wilby et al.

(2002) for assessing the impact of local climate change using statistical downscaling. This model was downloaded from the website http://co-public.lboro.ac.uk/cocwd/SDSM/. We used the output of CanESM2 as the predictor, and RCP 2.6, 4.5, and 8.5 were used for the generation of future data.

SDSM establishes the empirical relationship function (F) in Eq. (1) between the predictors and predictands. The model has four main parts: identification of the predictands and predictors, model calibration, weather generation, and generation of a future series of climatic variables (scenario generation). The quality-control module in SDSM can assess the performance of the predictands (precipitation and temperature) to identify errors, missing data, and outliers in the data records. We applied a transformation of the fourth root to account for the skewed nature of the rainfall distribution (Hassan et al., 2014). Some parameters such as threshold event, bias correction and variance inflation were adjusted several times during the calibration of SDSM until the statistical agreement between the observed and simulated outputs was highest for precipitation. The SDSM default values for these parameters were then used for temperature. The unconditional process and the monthly model were applied for temperature, and a conditional process was applied for precipitation. In an unconditional process it is assumed that there is a direct link between predictor and predictand and whereas conditional assumes the existence of intermediate processes between regional forcing and local weather.

*2.2.2.2. Downscaling daily rainfall and temperature time series*. Daily precipitation and maximum and minimum temperature were chosen as the predictand variables for the downscaling experiments. Precipitation and temperature have been measured at the Medenine meteorological station near our study area for 32 years (1978–2010). The large-scale predictor variables representing the current climatic conditions were derived from the reanalysed NCEP data for 1961 – 2005. To make a consistent data set of predictand and predictor variables we assumed the data got the period from 1961 to 1978 as missing data and assigned -999 to them to be applicable with the SDSM program. The other climatic variables for the future scenarios were extracted from the CanESM2 location that was closest to the study area. Data were ultimately extracted for three periods of 30 years each from 2011 to 2100): the 20 s (2011–2040), 50 s (2041–2070), and 80 s (2071–2100).

*2.2.2.3. Calibration and validation of SDSM*. The first 30 of the 45 years of the current climatic data (1961–1990) were used for calibrating the regression models, and the remaining 15 years of data (1991–2005) were used for SDSM validation. SDSM calibration computes the parameters of multiple regression equations for a set of probable predictors and each predictand (Dibike and Coulibaly, 2005). The performance of the SDSM was evaluated using the coefficient of determination ($R^2$). $R^2$ is a comparison of the variance of the modelled data with the total variance of the observed data (Shrestha et al., 2015). The weather-generator module in SDSM was used for the validation. We then used the summary statistics and frequency analysis in SDSM to compare the observed and simulated climatological data for the 15 years (1991–2005).

*2.2.3. Water harvesting model (WHCatch)*

Hydrological models are mathematical formulations that can determine the volume of runoff leaving a watershed from the rainfall received by the watershed (Abdo et al., 2009). We applied the simple model WHCatch (Adham et al., 2016b) for 25 sub-catchments in the Oum Zessar watershed to assess the performance of the RWH techniques based on current and future climatic conditions. The change of water storage within the volume was calculated as the difference between total input and output. The water-balance equation of an area can be written in units of volume ($m^3$) as (Boers et al., 1986):

$$\Delta S = I - Q \tag{2}$$

where ΔS is the change in storage during a defined period of time, I is the inflow, and Q is the outflow, all in $m^3$.

Recognition of the various types of in- and outflow allows a more detailed water-balance equation:

$$\Delta S = Q_{runoff} + Q_{rainfall} + Q_{in} - Q_{out} - Q_{loss} \tag{3}$$

where $Q_{runoff}$ is the volume of runoff into the retention basin from the runoff area, $Q_{rainfall}$ is the rainfall in the retention basin, $Q_{in}$ is the volume of inflow from upstream catchment(s), $Q_{out}$ is the volume of overflow from the retention basin to the next catchment(s), and $Q_{loss}$ represents the losses by infiltration from the retention basin and the crop evapotranspiration. The Thornthwaite equation was applied to estimate the potential evapotranspiration in each sub-catchment (Xu and Singh, 2001):

$$ET = 16\left(\frac{L}{12}\right)\left(\frac{N}{30}\right)\left(\frac{10T_a}{I}\right)^{\propto} \tag{4}$$

Where ET is the potential evapotranspiration (mm/month), $T_a$ is the average daily temperature (° C, if this is negative use 0), N is the number of days in the month being calculated, L is the average day length (hours) of the considered month and α is a parameter that is calculated as:

$$\propto = (6.75 \times 10^{-7})I^3 - (7.71 \times 10^{-5})I^2 + (1.792 \times 10^{-2})I + 0.49239 \tag{5}$$

with

$$I = \sum_{i=1}^{12}\left(\frac{T_{ai}}{5}\right)^{1.514} \tag{6}$$

where I is the heat index which depends on the 12 monthly mean temperatures $T_{ai}$. The maximum crop evapotranspiration ($ET_c$) was calculated by:

$$ET_c = ET \bullet K_c \tag{7}$$

Where $K_c$ is the crop coefficient.

The output data of CanESM2 for the three representative climate scenario's RCP 2.6, 4.5 and 8.5 were used as input data for WHCatch and the output was compared with the results for the current climatic variables. The volume of water that could be harvested in each sub-catchment was calculated and presented for the current (baseline) 1981–2010 period and the future periods 2011–2040, 2041–2070, and 2071–2100 (similar periods of climatic scenarios).

To achieve the adaptive goal of RWH for the future climatic scenarios, we changed the spillway heights and flow directions to optimise the performance of the RWH structures and to improve the yield (water availability) of the RWH system under the future climatic conditions.

## 3. Results and discussion

Here we will first look at the results of downscaling the climate scenario's for the study area. These will then be applied in the rainwater harvesting model.

### 3.1. Statistical downscaling

SDSM 4.2 was applied to assess the impact of local climate change using a statistical downscaling technique. Four main steps were applied: the predictor variables were selected, the calibration and validation of SDSM were evaluated (second and third steps), and a series of future climatic variables (projection of temperature and precipitation) was generated.

*3.1.1. Selection of predictor variables*

The choice of predictor variables is a major problem in the development of statistical downscaling. The screening option in SDSM assists

**Table 1**
Selected set of predictor variables with their description, each predictor was selected based on the highest correlation (r) and smaller significance level (P) value with each predictand. For all combinations of predictor and predictand the P-variable had a value of 0.00.

| Predictand | Predictor | Predictor description | Partial *r* |
|---|---|---|---|
| $T_{max}$ | p500*gl* | 500 hPa Geopotential | 0.239 |
| | s500*gl* | 500 hPa Specific humidity | −0.099 |
| | shum*gl* | 1000 hPa Specific humidity | −0.470 |
| | temp*gl* | Air temperature at 2 m | 0.841 |
| $T_{min}$ | p500*gl* | 500 hPa Geopotential | −0.077 |
| | s500*gl* | 500 hPa Specific humidity | 0.114 |
| | shum*gl* | 1000 hPa Specific humidity | 0.252 |
| | temp*gl* | Air temperature at 2 m | 0.700 |
| Precipitation | p1_ug*l* | 1000 hPa Zonal wind component | 0.104 |
| | p8_ug*l* | 850 hPa Zonal wind component | −0.180 |
| | prcp*gl* | Total precipitation | 0.199 |

in choosing the appropriate predictor variables for downscaling. The predictor variables from the reanalysed NCEP/NCAR (1961–2005) data were chosen to investigate the percentage of variance explained by each predictand-predictor pair. The final set of predictor variables was selected after analysing the significance level (P) and correlation coefficient (partial *r*), where each predictor was selected based on the highest correlation and smaller P value with each predictand (Table 1).

The procedure for selecting the predictor variables was similar to that used in other studies (Wilby et al., 2002; Dibike and Coulibaly, 2005; Hassan et al., 2014). Air temperature at a height of 2 m was the dominant predictor variable for both maximum and minimum temperature (Table 1). This variable has the highest impact on temperature and is expected to generate a temperature in response to a climatic scenario (Hassan et al., 2014). Total precipitation was the dominant predictor variable for precipitation. Some predictor variables (e.g. p1_ug*l*) were poorly correlated with precipitation (r = 0.104) but were selected because combinations of one or more of them were able to describe the conditional process for precipitation. The selection of predictor variables for maximum and minimum temperature was easier than for the rainfall predictor variables, because rainfall is under condition process.

### 3.1.2. SDSM performance

SDSM performance was evaluated by downscaling the temperature and precipitation for the study area. The calibration module in SDSM was applied automatically to evaluate the performance of SDSM using $R^2$ for the first 30 years (1961–1990). The $R^2$ values were 0.74, 0.64, and 0.28 for maximum temperature ($T_{max}$), minimum temperature ($T_{min}$), and precipitation (Prcp), respectively. These results indicated that SDSM performed well for downscaling maximum and minimum temperature but not for precipitation, which was more complex than temperature (Fowler et al., 2007). The complexity of downscaling rainfall is due to the conditional process, which is dependent on another intermediate process inside the rainfall process, such as humidity, cloud cover, and/or wet days (Hassan et al., 2014).

The weather-generator module in SDSM was used for validation. The observed data and results of the climatic simulation were then compared using summary and frequency analysis in SDSM for 1991–2005 (Fig. 2). Comparisons of the monthly mean maximum and minimum temperatures and precipitation indicated a good agreement between the observed and simulated outputs for $T_{max}$ and $T_{min}$, which were very similar.

The precipitation data, however, differed more, especially in March and August. The $R^2$ values were 0.97, 0.95, and 0.46 for $T_{max}$, $T_{min}$, and precipitation, respectively. These results indicated that SDSM performed well for the validation but not for the calibration of precipitation, perhaps due to missing rainfall data (observed), which negatively affected the performance of SDSM. Overall, the agreement between the observed and simulated monthly $T_{max}$, $T_{min}$, and Prcp was satisfactory.

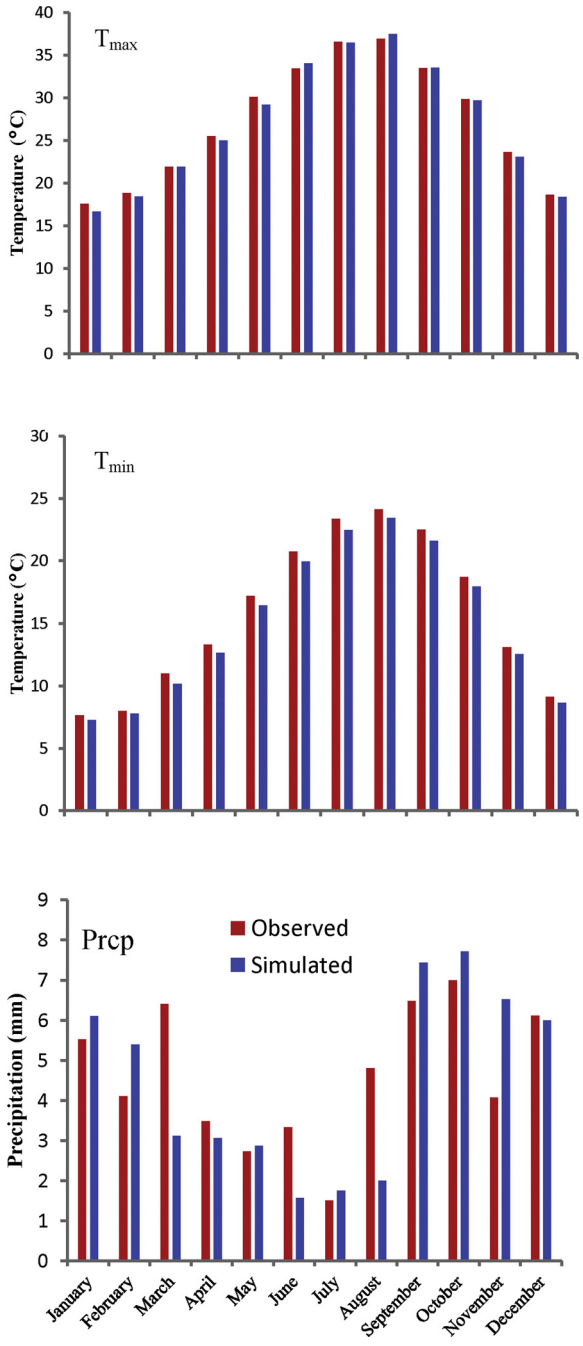


**Fig. 2.** Validation of SDSM performance for maximum temperature ($T_{max}$), minimum temperature ($T_{min}$), and precipitation by comparing the monthly means for the observed and simulated data for 1991–2005.

### 3.1.3. Projection of temperature and precipitation

The next step after validation was to use SDSM 4.2 to downscale the future scenario of climate change simulated by GCM. As explained above, the output from CanESM2 provided the predictors used in this study. The future climatic variables for RCP 2.6, 4.5, and 8.5 based on the mean of 20 ensembles were analysed for each 30-year period, i.e. 20 s (2011–2040), 50 s (2041–2070), and 80 s (2071–2100). The data for the baseline period (1981–2010) were compared with the future data. The downscaled maximum and minimum temperatures clearly indicated an increasing trend in the mean monthly temperature for all three scenarios and all future periods (Fig. 3).

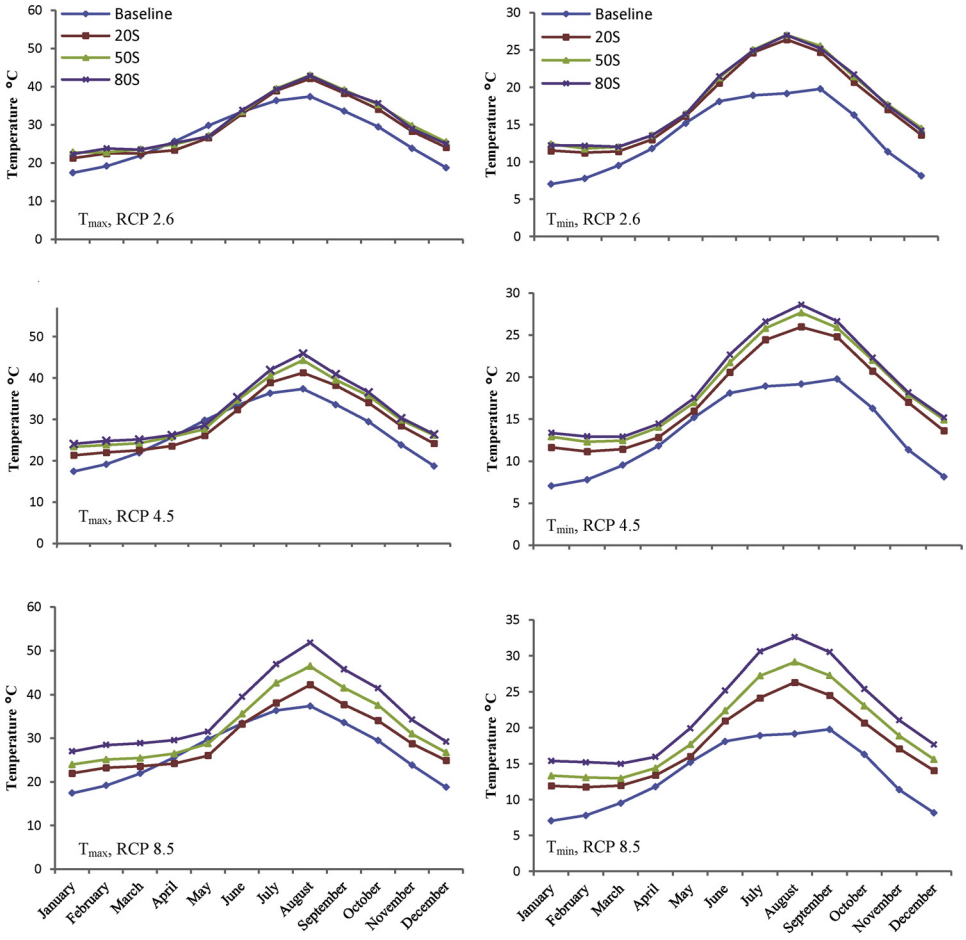


**Fig. 3.** Monthly mean maximum and minimum temperature under three scenarios (Representative Concentration Pathway 2.6, 4.5, and 8.5) in the baseline and the three projected periods (20 s, 50 s, and 80 s). The downscaled maximum and minimum temperatures clearly indicated an increasing trend in the mean monthly temperature for all three scenarios and all future periods.

**Table 2**
The mean annual maximum temperature ($T_{max}$), minimum temperature ($T_{min}$), precipitation and evapotranspiration and their predicted increase for the three scenarios in the three periods.

| | *RCPs* | 20 s | 50 s | 80 s |
|---|---|---|---|---|
| **$T_{max}$ ($^0$C)** | ***2.6*** | +2.33 | +3.32 | +3.29 |
| | ***4.5*** | +2.18 | +4.08 | +4.95 |
| | ***8.5*** | +2.61 | +5.39 | +8.96 |
| **$T_{min}$ ($^0$C)** | ***2.6*** | +3.98 | +4.63 | +4.61 |
| | ***4.5*** | +3.92 | +5.13 | +5.70 |
| | ***8.5*** | +4.13 | +5.98 | +8.45 |
| **Precipitation** | ***2.6*** | −27 | −37 | −29 |
| **(%)** | ***4.5*** | −30 | −33 | −30 |
| | ***8.5*** | −36 | −32 | −36 |
| **Evapotranspiration** | ***2.6*** | +6 | +8 | +8 |
| **(%)** | ***4.5*** | +6 | +10 | +12 |
| | ***8.5*** | +7 | +13 | +21 |

The mean annual maximum temperature under RCP 2.6 increased by 2.33 and 3.32 °C in the 20 s and 50 s periods, respectively. The increase in the mean annual maximum temperature was slightly lower at 3.29 °C by the end of this century compared with the 50 s period. The mean annual temperature increased in RCP 4.5 in all three periods. The increases in the maximum future temperatures were highest in RCP 8.5: 2.61 °C in 20 s, 5.39 °C in 50 s, and 8.96 °C in 80 s (Table 2). RCP 8.5 assumed higher emissions of greenhouse gases than RCP 4.5 (Rajesh, 2015), and RCP 2.6 usually assumed the lowest emission due to mitigate activities (Van Vuuren et al., 2011). The mean annual maximum temperature increased in all months, except in May when the temperature was slightly lower for all scenarios in all periods. Temperature only increased in May in RCP 8.5 for the 80 s period (Fig. 3).

The mean annual minimum temperature also increased in all three scenarios in all periods and months (Table 2). The mean annual minimum temperature increased in RCP 2.6 by 3.98 °C in 20 s and by 4.63 °C in 50 s, and the increase was slightly lower at 4.61 °C by the end of this century, as with the maximum temperature. The mean annual minimum temperature increased in RCP 4.5 during all periods. The minimum temperature increased most in RCP 8.5: 4.13, 5.98, and 8.45 °C in 20 s, 50 s, and 80 s, respectively (Table 2 and Fig. 3). Mean annual minimum temperature increased substantially during summer (June-September), especially in RCP 8.5, but increased only slightly in May.

The increases in the mean maximum and minimum temperatures were generally slightly higher than those in earlier studies (MARH, 2011), but our results are consistent with an increasing trend for the 21$^{th}$ century. This study is the first to apply new scenarios based on CMIP5 modelling to this region.

Potential evapotranspiration is projected to increase in the future due to the impact of increasing temperatures (Fig. 4a). Monthly ET-values show a similar pattern in all three scenarios, but RCP 8.5 increases more than the other two scenarios, especially during June to September. The annual mean potential ET is likely to increase by 6% in RCP 2.6 in 20 s to 21% in RCP 8.5 in 80 s (Table 2).

The projection for precipitation indicated a decreasing trend in the mean annual daily precipitation for the three scenarios in all periods (Fig. 4b). The mean annual daily precipitation decreased in RCP 2.6 by 27% in 20 s, 37% in 50 s, and 29% in 80 s and in RCP 4.5 by about 30% in 20 s and 80 s and by 33% in 50 s. The mean annual daily precipitation decreased most in RCP 8.5, by 36% in both 20 s and 80 s and by about 32% in 50 s (Table 2). These changes in precipitation varied monthly. The largest decrease was in March and October in all

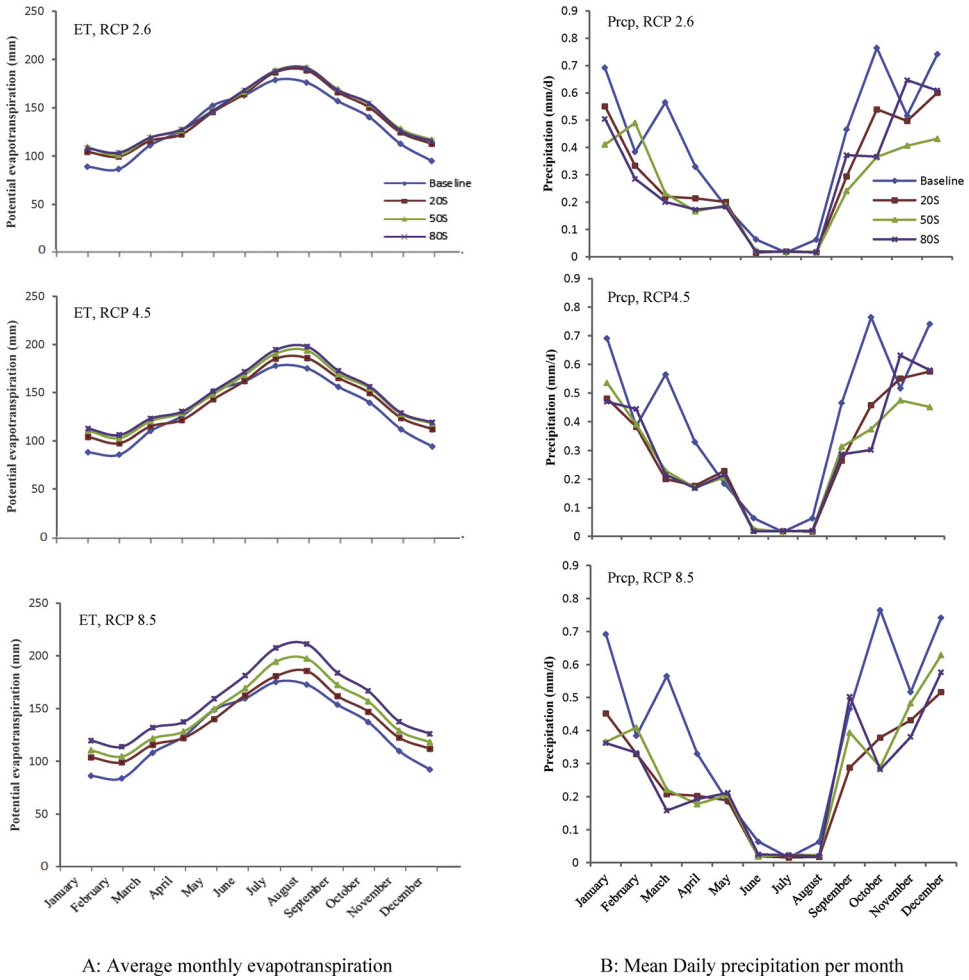


**Fig. 4.** Monthly mean evapotranspiration (a) and monthly mean precipitation (b) in the three scenarios Representative Concentration Pathway (RCPs) in the baseline and the three projected periods.

scenarios and periods. The mean annual daily precipitation increased slightly in RCP 2.6 in February 50 s, in RCP 4.5 in February 80 s and November 80 s and 20 s, and in RCP 8.5 in May and September 80 s (Fig. 4b). The pattern was similar in RCP 2.6 and 4.5 but with some differences, whereas the pattern was much different in RCP 8.5 in September to December in 20 s and 80 s compared with the base.

These results are generally consistent with the climatic projections in a Tunisian case study, which reported that rainfall would decrease between 10% in the north and 30% in the south in the same period (MARH, 2011).

To gain more insight in the predicted precipitation and the expected changes, the generated RCP4.5 dataset was analysed and compared with the baseline precipitation period of 1981–2010. To do so, first the distribution of the daily amounts of precipitation was computed. The cumulative probabilities are shows in Fig. 5a.

Fig. 5a, shows that the probability of a day with rainfall was only 7% for the years 1981–2010, while the probability increases to 16, 14 and 14% for the periods 2011–2040, 2041–2070 and 2071–2100 respectively. The chance of a rainfall event of 2.5 mm or more is 3, 1.8, 1.5 and 1.9% for the different periods. The larger the amount of precipitation, the smaller the differences between the periods.

Not only the size of the precipitation events is important, so is the number of them. For every year considered we counted the number of events. Classes of precipitation of 10 mm were assumed and the number of events was counted for each class during the four periods considered. The results of this simple but effective analysis are shown in Fig. 5b. From this figure it can be seen that during the years 1981–2010 the majority of years had between 30–40 precipitation events. During this period there were also years with 0–10 events. In the periods with generated data, there were no years with less than 30 events. During 2041–2070 and 2071–2100 no years occurred with more than 80.

The projection results of temperature, evapotranspiration and precipitation were used in the WHCatch model to estimate the future water availability in each sub-catchment. The amount of rainfall and the change in temperature directly affected the evapotranspiration values and the water balance terms.

### 3.2. Water harvesting model (WHCatch)

The WHCatch model was used to estimate future water availability for each RWH structure relative to the baseline period. The sub-catchments and flow directions are shown in Fig. 6.

The amount of water that will be caught by each RWH structure is highly dependent on the amount of precipitation in its sub-catchment and on the actual evapotranspiration. Changes in precipitation and temperature will therefore have a direct impact on the availability of water and on the performance of RWH in general. The simulations for each sub-catchment for RCP 2.6, 4.5, and 8.5 for the 20 s (2011–2040), 50 s (2041–2070), and 80 s (2071–2100) are compared with the baseline period (1981–2010) and presented in Fig. 7a.

The volume of water stored in a reservoir depends on the available runoff and the water demand. The performance of RWH under current conditions was previously assessed and discussed (Adham et al., 2016b). The amount of water stored in each sub-catchment decreased

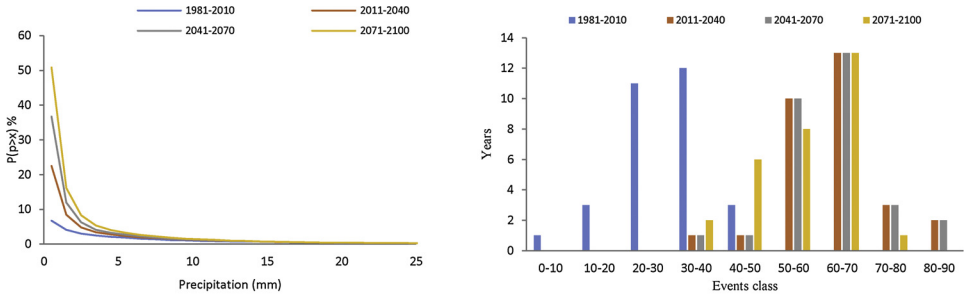


A: Precipitation Probability

B: Number of rainfall events per year

**Fig. 5.** The probability of precipitation events in the Representative Concentration Pathway (RCP4.5) scenario (a) and the number of years in which a certain number of rainfall events occur (b).

under the future conditions in RCP 2.6, 4.5, and 8.5 (Fig. 7a). The results of WHCatch were identical to those for projected precipitation (Fig. 4b). About 72% of the sub-catchments were able to meet the water requirements in the baseline period. For future scenarios about 30% in RCP 2.6, 25% in RCP 4.5 in all periods and 50% for RCP 8.5 in 20 s and 50 s will be able to meet the water requirements (Fig. 7a). Whereas, only 25% of the sub-catchments for 80 s in the RCP 8.5 able to meet the water requirements. Zero values of harvested rainwater for the sub-catchments, however, indicated the inability of RWH to meet the water requirements. The zero values were due to reasons such as insufficient storage capacity, suboptimal height of the spillway, direction of streamflow (Adham et al., 2016b).

The watershed-runoff relationship in ASARs has long been reported. The volume of the harvested runoff is directly proportional to the size and length of the runoff-harvesting structure (Adham et al., 2018). Most of the RWH structures built by farmers in ASARs are washed away due to the insufficient capacity of spillways (Adham et al., 2016b). Spillways with sufficient capacity and at the right location must therefore be provided. Field observations and the analysis of the water balance indicated that most of the runoff flowed in one direction (Fig. 6a). Adham et al. (2016b) reported that changing spillway heights together with flow directions substantially increased rainwater availability under current climatic conditions for the proposed RWH solutions compared to the results for traditional designs. The analyses with WHCatch indicated that changing spillway heights together with flow directions (Fig. 6b) for optimising the performance of the RWH structures and improving the yield (water availability) of the RWH system based on the projected future climatic conditions (Fig. 7b) substantially increased the performance of RWH, increasing the efficiency of water availability in 92% of all sub-catchments in the baseline period in all three RCP scenarios compared to 72% without the changes. The efficiency of water availability will be increased almost double in both scenarios RCP 2.6 and 4.5 in all periods compared to the sub-catchments without changes, whereas the efficiency of water availability will be the same for 80 s in RCP 2.6. Moreover, about 80% of the sub-catchments in the RCP 8.5 in 20 s and 50 s will be able to meet the water requirements compared to 50% without the changes (Fig. 7b and Table 3). Fig. 8b shows that the first four RWH structure (sub-catchments) have no big significant change with this scenario. These results are due to a relatively small runoff area in the first three structures, whereas the structure was broken in the fourth site and we considered it works as a runoff area. Harvested rainwater increased in all three RCPs (Table 3). Table 3, confirmed that the increasing of the water supply in most sub-catchments are more depend on the water management and structure design than climate change scenarios itself.

## 4. Conclusions

This study demonstrated the feasibility of rainwater harvesting as an adaptive strategy to mitigate water scarcity and to improve water availability now and under changing climatic conditions. Analysing our generated data showed that both the minimum and maximum temperatures tended to increase and precipitation tended to decrease in all scenarios of future emissions of greenhouse gases in most periods (20 s, 50 s, and 80 s). The increase in temperature yields an increase in potential evapotranspiration as well. Changing the flow directions combined with increasing the heights of spillways had a large impact on the performance of the rainwater harvesting structures. Water availability

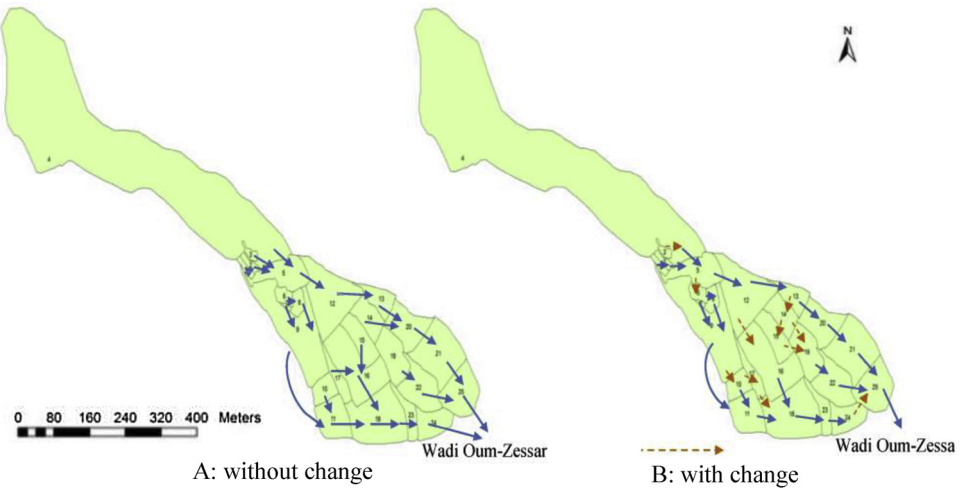


A: without change

B: with change

**Fig. 6.** Study area with normal flow directions (a) and changed flow directions (b).

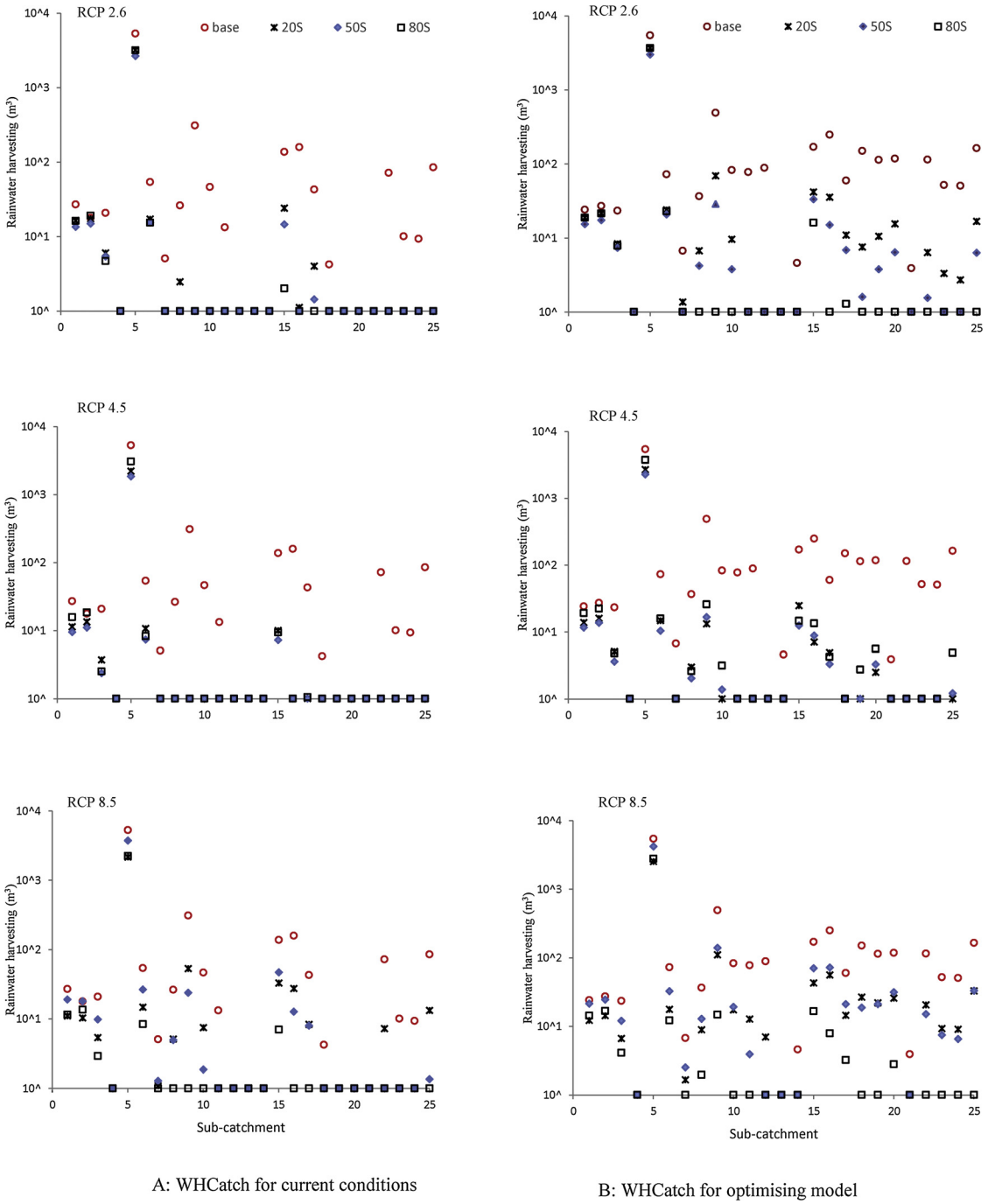


**Fig. 7.** Results of water-harvesting modelling. The simulation of harvested rainwater in each sub-catchment under normal conditions (a) and the results after optimisation of the rainwater harvesting system (b).

**Table 3**
The efficiency (%) of water availability in all sub-catchments in present and future climate scenarios, comparing normal situation and changing spillway hights together with flow direction (optimisation).

| | Efficiency under current condition (%) | | | Efficiency under adjusted condition (%) | | |
|---|---|---|---|---|---|---|
| Baseline | 72 | | | 92 | | |
| | 20S | 50S | 80S | 20S | 50S | 80S |
| **RCP 2.6** | 36 | 28 | 24 | 76 | 64 | 28 |
| **RCP 4.5** | 24 | 24 | 24 | 44 | 52 | 56 |
| **RCP 8.5** | 56 | 52 | 24 | 84 | 80 | 44 |

fulfilled the demand in 92% of the sub-catchments compared to only 72% without these adaptive measures in all the scenarios of climate change. Therefore, at sub-catchments level, water management and structure design play a more important role in the performance of rainwater harvesting rather than climate change itself.

The results could be important for designers, decision-makers, and farmers for adapting to the forthcoming climatic conditions and/or for mitigating the adverse impacts of a changing climate on water resources. Further research, however, is required to include multiple general circulation models (GCMs) and downscaling models under Coupled Model Intercomparison Project (CMIP5) and to consider changes in land use/cover in simulation models to better understand the impact of climate change on water availability.

## Acknowledgments

This study was conducted as part of a PhD programme, with co-operation between The Higher Committee for Education Development in Iraq (HCED) and Wageningen University (The Netherlands). The field work was carried out in collaboration with the Institute des Régions Arides (*IRA*) in Tunisia. Many thanks go to Klaas Oostindie at Wageningen University for preparing the figures. This study was part of the European Union's Seventh Framework Programme (FP7/2007-2013, WAHARA project). We are thankful to the anonymous reviewers and the editor for their constructive comments and suggestions on the manuscript.

## References

Abdo, K.S., Fiseha, B.M., Rientjes, T.H.M., 2009. Assessment of climate change impacts on the hydrology of Gilgel Abay catchment in Lake Tana basin, Ethiopia. Hydrol. Process. 23, 3661–3669. https://doi.org/10.1002/hyp.7363.

Abouabdillah, A., 2010. Hydrological Modeling in a Data-poor Mediterranean Catchment (Merguellil, Tunisia). Assessing Scenarios of Land Management and Climate Change. PhD Thesis. Tuscia University Of Viterbo, Italy 148 pp.

Adham, A., Riksen, M., Ouessar, M., Ritsema, C.J., 2016a. A methodology to assess and evaluate rainwater harvesting techniques in (Semi-) arid regions. Water 8, 198.v. https://doi.org/10.3390/w8050198.

Adham, A., Wesseling, J.G., Riksen, M., Ouessar, M., Ritsema, C.J., 2016b. A water harvesting model for optimizing rainwater harvesting in the wadi Oum Zessar watershed, Tunisia. Agric. Water Manag. 176, 191–202. https://doi.org/10.1016/j.agwat.2016.06.003.

Adham, A., Sayl, K.N., Abed, R., Abdeladhim, M.A., Wesseling, J.G., Riksen, M., Ritsema, C.J., 2018. A GIS-based approach for identifying potential sites for harvesting rainwater in the Western Desert of Iraq. Int. Soil Water Conserv. Res. 6 (4), 297–304.

Al-Ansari, N., Abdellatif, M., Ali, S.S., Knutsson, S., 2014. Long term effect of climate change on rainfall in northwest Iraq. Cent. Eur. J. Eng. 4, 1–14. https://doi.org/10.2478/s13531-013-0151-4.

Ammar, A., Riksen, M., Ouessar, M., Ritsema, C.J., 2016. Identification of suitable sites for rainwater harvesting structures in arid and semi-arid regions: a review. Int. Soil Water Conserv. Res. 4 (2), 108–120. https://doi.org/10.1016/j.iswcr.2016.03.001.

Boers, T.M., Zondervan, K., Ben-Asher, J., 1986. Micro-Catchment-Water-Harvesting (MCWH) for arid zone development. Agric. Water Manag. 12, 21–39. https://doi.org/10.1016/0378-3774(86)90003-X.

Chiew, F.H.S., Whetton, P.H., McMahon, T., Pittock, B., 1995. Simulation of the impacts of climate change on runoff and soil moisture in Australian catchments. J. Hydrol. 167, 121–147. https://doi.org/10.1016/0022-1694(94)02649-V.

Dibike, Y.B., Coulibaly, P., 2005. Hydrologic impact of climate change in the Saguenay watershed: comparison of downscaling methods and hydrologic models. J. Hydrol. 307, 145–163. https://doi.org/10.1016/j.jhydrol.2004.10.012.

Fowler, H., et al., 2007. Ocean circulation: thermohaline circulation. Encycl. Atmos. Sci. 4, 1549–1555. https://doi.org/10.1002/joc.

Grotch, S.L., MacCracken, M.C., 1991. The use of general circulation models to predict regional climatic change. J. Clim. 4, 286–303. https://doi.org/10.1175/1520-0442(1991)004<0286:TUOGCM>2.0.CO;2.

Hassan, Z., Shamsudin, S., Harun, S., 2014. Application of SDSM and LARS-WG for simulating and downscaling of rainfall and temperature. Theor. Appl. Climatol. 116, 243–257. https://doi.org/10.1007/s00704-013-0951-8.

IPCC, 2014. C. B., F. V.R. Barros D.J. Dokken K.J. Mach M.D. Mastrandrea T.E. Bilir M. Chatterjee K.L. EBI Y.O. Estrada R.C. Genova B. Girma E.S. Kissel A.N. Levy S. Maccracken P.R. Mastrandrea L.L. White Cambridge, United Kingdom and New York, NY, USA2014. Climate Change 2014: Impacts, Adaptation and Vulnerability. Contribution of Working Group II to the Fifth Assessment Report of the Intergovernmental Panel on Climate Change2014. C. B., F, Barros, V.R., Dokken, D.J., Mach, K.J., Mastrandrea, M.D., Bilir, T.E., Chatterjee, M., EBI, K.L., Estrada, Y.O., Genova, R.C., Girma, B., Kissel, E.S., Levy, A.N., Maccracken, S., Mastrandrea, P.R., White, L.L. (Eds.), 2014. Climate Change 2014: Impacts, Adaptation and Vulnerability. Contribution of Working Group II to the Fifth Assessment Report of the Intergovernmental Panel on Climate Change.

Ipcc-Tgic, A., 2007. General Guidelines on the Use of Scenario Data for Climate Impact andAdaptation Assessment. Version 2. From. http://www.ipcc-data.org/guidelines/TGICA_guidance_sdciaa_v2_final.pdf.

Lebel, S., Fleskens, L., Forster, P.M., 2015. Evaluation of in situ rainwater harvesting as an adaptation strategy to climate change for maize production in Eainfed Africa. Water Resour. Manag. 29, 4803–4816. https://doi.org/10.1007/s11269-015-1091-y.

Li, H., Zhao, X., Gao, X., Ren, K., Wu, P., 2018. Effects of water collection and mulching combinations on water infiltration and consumption in a semiarid rainfed orchard. J. Hydrol. 558, 432–441.

MARH, G., 2011. Stratégie Nationale D' Adaptation De L' Agriculture Tunisienne Et Des Écosystèmes Aux Changements Climatiques. Ministry of Infrastructure and Environment, Tunisia 148p.

Moss, R.H., Edmonds, J.A., Hibbard, K.A., 2010. The next generation of scenarios for climate change research and assessment. Nature 463, 747–756. https://doi.org/10.1038/nature08823.

Mukheibir, P., 2008. Water resources management strategies for adaptation to climate-induced impacts in South Africa. Water Resour. Manag. 22, 1259–1276. https://doi.org/10.1007/s11269-007-9224-6.

Rajesh, 2015. Potential impacts of climate change on hydrology of western siberian lowland catchments. Erasmus Mundus Master Sci. Ecohydrol. 72, 1–8.

Rind, D., Goldberg, R., Hansen, J., 1990. Potential evapotranspiration and the likelihood of future drought. J. Geophys. Res. 95, 9983–10004. https://doi.org/10.1029/JD095iD07p09983.

Setegn, S.G., Rayner, D., Melesse, A.M., 2011. Climate change impact on agricultural water resources variability in the Northern highlands of Ethiopia. In: Melesse, A.M. (Ed.), Nile River Basin: Hydrology, Climate and Water Use, 1st edn. Springer, pp. 241–265. https://doi.org/10.1007/978-94-007-0689-7_12. X, 480 p. 200 illus; part 4.

Shrestha, S., Anal, A.K., Salam, P.A., der Valk, M., 2015. Managing Water Resources under Climate Uncertainty. 438p. https://doi.org/10.1007/987-3-319-10467-6.

Taylor, K.E., Stouffer, R.J., Meehl, G.A., 2012. An overview of CMIP5 and the experiment design. Bull. Am. Meteorol. Soc. 93, 485–498. https://doi.org/10.1175/BAMS-D-11-00094.1.

Thomson, A.M., Calvin, K.V., Smith, S.J., Kyle, G.P., Volke, A., Patel, P., Delgado-Arias, S., Bond-Lamberty, B., Wise, Ma., Clarke, L.E., Edmonds, Ja., 2011. RCP4.5: a pathway for stabilization of radiative forcing by 2100. Clim. Change 109 (1), 77–94. https://doi.org/10.1007/s10584-011-0151-4.

Van Vuuren, D.P., Edmonds, J.A., Kainuma, M., 2011. A special issue on the RCPs. Clim. Change 109, 1–4. https://doi.org/10.1007/s10584-011-0157-y.

Wilby, R.L., Wigley, T.M.L., 2000. Precipitation predictors for downscaling: observed and general circulation model relationships. Int. J. Climatol. 20, 641–661. https://doi.org/10.1002/(SICI)1097-0088(200005)20:6<641::AID-JOC501>3.0.CO;2-1.

Wilby, R.L., Dawson, C.W., Barrow, E.M., 2002. SDSM—a decision support tool for the assessment of regional climate change impacts. Environ. Model. Softw. 17, 145–157. https://doi.org/10.1016/S1364-8152(01)00060-3.

Xu, C., 1999. Climate change and hydrologic models: a review of existing gaps and recent research developments. Water Resour. Manag. 13, 369–382. https://doi.org/10.1023/A:1008190900459.

Xu, C.Y., Singh, V.P., 2001. Evaluation and generalization of temperature based methods for calculating evaporation. Hydrol. Process. 15 (2), 305–319. https://doi.org/10.1002/hyp.119.